PHILOSOPHICAL TRANSACTIONS OF THE ROYAL SOCIETY A MATHEMATICAL, PHYSICAL & ENGINEERING SCIENCES

Ignition of fires

Arvind Atreya

Phil. Trans. R. Soc. Lond. A 1998 **356**, 2787-2813
doi: 10.1098/rsta.1998.0298

THE ROYAL SOCIETY

Ignition of fires

By Arvind Atreya

Department of Mechanical Engineering and Applied Mechanics, University of Michigan, Ann Arbor, MI 48109, USA

This paper discusses the mechanisms that lead to ignition of fires and the reasons behind the experimental correlations available in the literature. The objective is to understand and quantify the physics of heat and mass transfer and the chemistry of solid-phase decomposition and gas-phase runaway reactions that result in the appearance of a sustained gas-phase diffusion flame—a phenomenon identified as ignition. Both *spontaneous* (auto) and *piloted* (forced) ignition phenomena are discussed. Two types of materials commonly found in building fires are considered—thermoplastics that melt and vaporize upon heating, and cellulosic materials that decompose and produce char. A general theoretical model is derived and specific numerical and analytical solutions are discussed in the light of experimental evidence and data. It is concluded that within the approximation of constant surface temperature at ignition, the ignition delay data may be correlated by a simple thermal model based on inert heating of the solid. However, a significantly more complicated description which includes gas and solid-phase chemistry is required if the surface temperature at ignition is not constant.

Keywords: fires; piloted ignition; spontaneous ignition; thermal decomposition; experimental correlations; models; diffusion flames

1. Introduction

Ignition refers to the marked transition of a system from a non-reactive equilibrium state to a self-sustaining reactive state. This change is often induced by an external stimulus (such as heat or a spark) that produces a thermochemical runaway in the system. The subject of ignition is fundamental to combustion science and of great practical importance. It has, therefore, been intensely investigated since the days of van't Hoff and le Chatelier. Ignition has been studied both from the point of view of initiating desired combustion (such as in automobile, turbine and rocket engines) and preventing undesired combustion (such as in accidental fires). The disastrous consequences of an aircraft turbine ignition failure in mid-air, or a high-rise building fire are self-evident. From the fire safety perspective, of concern here, ignition is important not only because it is initiation of a fire, but also because it plays a critical role in fire growth. The spread of fire between objects in a room or between buildings is an ignition process. Even flame spread over continuous fuel surfaces is a continuous ignition process in which the adjacent flame serves both as a source of heat and as an igniting pilot.

The flammable world surrounding us contains a large variety of combustible materials (solids, liquids and gases) and oxygen is ever present. To focus on the most common fire scenario, this work limits itself to ignition of combustible solids. Two types of solids that are commonly encountered in a fire are considered: (i) cellulosics (such

as wood, paper, cotton, etc.) and (ii) thermoplastics (such as the frequently studied polymethylmethacrylate (PMMA)). The objective is to understand the mechanisms and conditions that lead to a sustained appearance of a flame in the gas phase when a combustible solid is heated by an external source. Two types of ignition are possible under these conditions: *spontaneous* (auto) and *piloted* (forced). This depends on whether the ignition occurs with or without the aid of an external pilot such as a spark or a flame. From the fire research perspective, piloted ignition is more important because: (i) it occurs at a lower threshold; (ii) it is the mechanism responsible for fire growth; and (iii), in practice, it is usually impossible to exclude all possible external pilot sources.

A substantial amount of research has been done on both spontaneous and piloted ignition and several excellent reviews have been presented by Welker (1970), Kanury (1972, 1988), Steward (1974) and Drysdale (1985). This paper will briefly review the general phenomena associated with ignition caused by external heating and will primarily focus on quantifying the physics of heat and mass transfer and the chemistry of solid phase decomposition and gas phase runaway reactions that lead to ignition. Since the theoretical formulations are comparatively simpler for spontaneous ignition, it is discussed first, and later the more practical piloted ignition problem is addressed.

2. Summary of experimental methods and observations

Experimentally, ignition is marked by the appearance of a sustained diffusion flame in the volatile gas stream evolved from a solid exposed to an external heat source. In building fires, typical heat sources are (i) direct convective heating from hot gases or flames; and/or (ii) thermal radiation from the surrounding flames, the ceiling layer of hot gases and hot walls. Ignition by direct convective heating of objects by flames and hot gases results in flame spread over the objects and the rate of this flame spread may be determined by computing the rate of the advancing piloted ignition front (Quintiere 1981; Atreya 1983*a*; Drysdale 1985; Mekki *et al*. 1990; Agrawal & Atreya 1992). Since the data from radiative ignition studies successfully predict the flame spread rate, the fundamental ignition property of materials is independent of the mode of heat transfer to the object (convective and/or radiative). Given this equivalence and the fact that most ignition studies are conducted by using a radiative heat source, this work presumes, for discussion purposes, the existence of an external radiation source.

From the point-of-view of flame spread and fire safety in general, the quantity of greatest interest is the time it takes from the commencement of heating to the onset of sustained flaming. To determine this time for different materials and to identify the critical conditions at ignition, several experimental investigations have been conducted and standard test methods have also been developed (ASTM 1990*a*, *b*; ISO 1990; Babrauskas & Parker 1987; Quintiere & Harkleroad 1984).

(*a*) *Experimental methods*

Experimental investigation of the ignition phenomenon requires: (i) a suitable heat source to simulate the fire heat flux; (ii) a method of mounting and exposing the sample to the heat source; and (iii) a pilot for piloted ignition studies. Various

experimental techniques differ from each other in these three areas and in the measurements made. Commonly used heat sources are gas-fired radiant panels (Simms 1960, 1961, 1962, 1963; Simms & Law 1967; Robertson *et al*. 1956; Quintiere *et al*. 1983); high-temperature tungsten filament lamps (Smith & King 1970; Wesson *et al*. 1971); flame (Bamford *et al*. 1946; Koohyar *et al*. 1968); flow furnaces for convective ignition studies (Weatherford & Sheppard 1965); carbon arc (Martin 1965); CO_2 laser (Kashiwagi 1979, 1981); and electrical heaters (Atreya 1983*a*; Deepak & Drysdale 1983; Janssens 1991). The samples are either mounted in the horizontal or the vertical configuration and a small flame (Atreya *et al*. 1986), or a heated wire (Akita 1959), or an electrical spark (Janssens 1991) is used as a pilot. Nearly all the investigators have measured the time required for ignition, but the measurements have not always been in good agreement. A few investigators have also measured the temperature of the solid surface exposed to the incident heat flux, either by using surface thermocouples (Kashiwagi 1981; Atreya 1983*a*; Deepak & Drysdale 1983; Thomson & Drysdale 1987) or by infrared pyrometers (Smith & King 1970). Others have estimated the surface temperatures either by extrapolating temperatures measured in depth (Martin 1965) or by using a linear heat conduction theory (Simms & Law 1967). Very few investigators (Deepak & Drysdale 1983; Drysdale & Thomson 1989; Atreya & Abu-Zaid 1992) have measured the fuel mass flux evolved from the solid surface during ignition.

(*b*) *Ignition criteria*

The data collected in the ignition experiments are correlated to deduce an empirical ignition criterion. Several criteria such as: critical solid surface temperature at ignition (Akita 1959; Simms & Law 1967; Thomson *et al*. 1988); critical fuel mass flux (Bamford et al. 1946; Akita 1959; Drysdale & Thomson 1989); critical char depth (Sauer 1956); critical mean solid temperature (Martin 1965); etc., have been proposed. Of these, critical fuel mass flux at ignition is physically the most correct, but surface temperature has proved to be the most useful, since it can be conveniently related to fire spread (Quintiere *et al*. 1983; Atreya 1983*a*; Drysdale 1985; Quintiere 1995). It is important to note that the above criteria are indirect quantities assumed to be closely related to the ignition event. The actual process as described in § 3 is quite complex. The solid must first chemically decompose to inject fuel gases into the boundary layer. These fuel gases must then mix with the surrounding air to produce a flammable mixture which is ignited either spontaneously or with the help of a pilot. For spontaneous ignition it is also necessary that the temperature of the flammable mixture be sufficiently high to initiate and accelerate the gas-phase exothermic chemical reactions. Further, for sustained ignition the fuel production rate must be such that the heat released by the nascent flame is sufficient to overcome the heat losses, otherwise only a flash is obtained. Thus, to obtain a rational criteria for sustained ignition, Rasbash & Drysdale (1983) proposed that a diffusion flame will persist in the gas phase only if the convective heat losses from the flame to the colder fuel surface do not exceed a certain fraction of the heat released by the flame. This fact was later used by Rasbash *et al*. (1986) and Atreya & Wichman (1989) to obtain the critical heat and mass transfer conditions at piloted ignition.

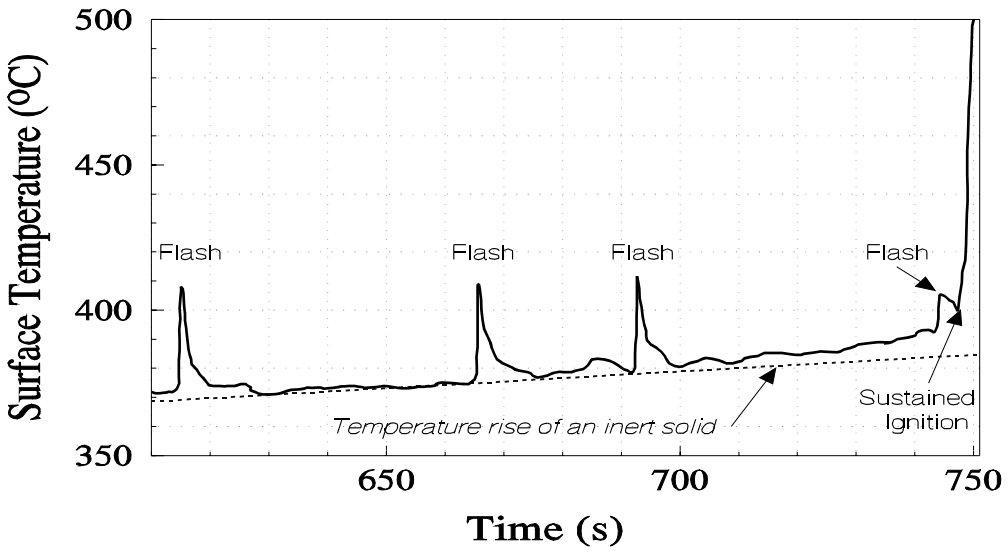

Figure 1. An enlarged view of the measured surface temperature–time-history during flashes and sustained ignition for a piloted ignition experiment on a horizontal red oak sample exposed to 18.8 kW m^{-2} external heat flux.

(*c*) *Experimental observations*

It is instructive to examine in detail the exposed surface temperature history prior to ignition. The solid line in figure 1 shows the chart recorder trace of the measured surface temperature during the last few instants of sustained piloted ignition. The sharp peaks in the surface temperature prior to sustained ignition are due to flashes (momentary unsustained flaming). While flashes are almost always observed during piloted ignition experiments, their effect on the solid surface temperature is difficult to record either because they do not occur right above the thermocouple or because the thermocouple is too deeply imbedded into the surface so that its time response is poor. Thus, figure 1 shows a rare occurrence; one out of more than one hundred experiments conducted by Atreya (1983*a*). Even in this experiment, all the flashes did not occur directly over the thermocouple and hence were not recorded. Also, for high heat fluxes the flashes may be too close together to be indistinguishable from the ignition event.

The dashed line in figure 1 shows the hypothetical temperature rise of an inert solid with the same physical properties as red oak and exposed to the same external radiation. A comparison of the dashed line with the measured surface temperature shows that for this low heat flux experiment, there was sufficient time between the flashes for the surface to come to thermal equilibrium with the external radiation. Also, the total heat contribution to the solid because of the flashes (proportional to the area under the peak) is small compared to that due to external radiation and is quickly lost by reradiation. Thus, *while the heat lost by the flame to the solid at the instant of ignition is significant (and may cause thermal quenching, resulting in a flash), its contribution to the enthalpy rise of the solid is negligible and critical conditions for ignition are achieved primarily by external radiant heating.* It is also important to note that the measured surface temperature (*ca.* 400 °C) and the hypothetical inert solid surface temperature (*ca.* 384 °C) at the time of sustained

ignition (747 s) is less than the momentary rise in temperature caused by the flashes and yet sustained flaming was not achieved. In other words, for sustained flaming to occur, it is necessary for the surface temperature, caused by external radiation, to rise to some critical value such that critical pyrolysate mass flux is generated by the solid, as suggested by Rasbash & Drysdale (1983) and Rasbash *et al*. (1986). If contributions due to gas-phase exothermicity are included in determining this critical value the accordance between the more physical critical mass flux criteria and the simpler surface temperature criteria is violated. Thus, in the present example, the critical surface temperature at ignition should be taken as 384 °C and not 400 °C. This observation is important because it simplifies the theoretical determination of the critical surface temperature and provides insight into the ignition process.

3. Chemical and physical ignition processes

For ignition to occur, a sequence of chemical and physical events must take place, starting with the solid-phase thermal decomposition and ending with the gas-phase thermal explosion resulting in a flame. These events are summarized in this section with the objective of developing an appropriate theoretical model and are based on previous experimental investigations. These investigations show that the measured time to ignition is affected by several factors that may be classified as internal or external to the solid. The external factors (environmental variables) are as follows. (i) The temperature, composition and velocity of the gas flow around the solid sample (Abu-Zaid 1988). The flow may be forced or buoyantly generated. For buoyantly generated flow, the orientation of the sample (actually, the orientation of the surface exposed to external heat) relative to gravity is important (Kashiwagi 1982; Atreya *et al*. 1986). (ii) The magnitude, uniformity and spectral quality of the incident radiation relative to the spectral absorptivity of the exposed sample surface and the spectral transmittance of the decomposition products (Welker 1970; Wesson *et al*. 1971). Due to significant absorption of incident radiation by the decomposition products (Kashiwagi 1981), their flow direction relative to the direction of incident radiation is also important. (iii) The sample geometry, sample thickness and the size of the exposed area (Simms & Law 1967). (iv) For piloted ignition, the location and size of the pilot relative to the ignition surface is also important (Simms 1963). Factors internal to the sample are (i) the thermophysical and thermochemical properties of the solid and its moisture content (Simms & Law 1967; Atreya 1983*a*; Janssens 1991); (ii) radiative properties of the exposed surface such as spectral absorptivity and transmissivity (Wesson *et al*. 1971; Kashiwagi 1981); and (iii) kinetics of thermal decomposition (Alvares & Martin 1971). It seems that poor agreement between various experimental studies is caused by the lack of control of some or all these variables.

Figure 2 schematically summarizes the following chemical and physical processes occurring during ignition.

(1) Heat transfer to the solid from an external source by convection and/or radiation. The net heat flux arriving at the solid surface should include attenuation of external radiation due to gas-phase absorption. Contributions due to exothermic gas-phase reactions should be included in the solid-phase energy balance only if they are known to be significant. Heat lost by the exothermic gas-phase reactions to the solid

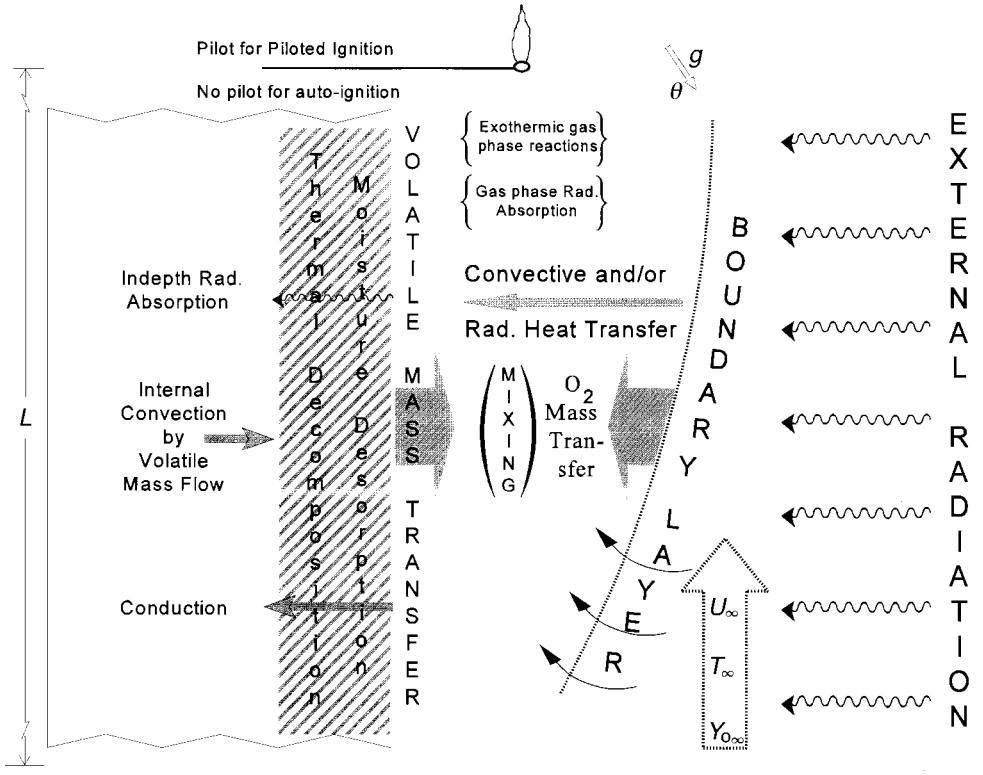

Figure 2. A schematic diagram of the chemical and physical processes occurring during ignition.

is, however, significant for the gas-phase energy balance and may thermally quench them.

(2) The fraction of the incident radiative heat flux absorbed by the solid depends on the spectral absorptivity and transmissivity of the solid and the spectral character of the incident radiation. Once absorbed, heat transfer within the solid occurs primarily via conduction.

(3) After the commencement of external heating, temperatures throughout the solid gradually increase, being highest at or near the surface. Prior to the decomposition of the surface layer, evaporation of moisture occurs and a moisture evaporation zone begins to travel into the solid. (Moisture evaporation is typical for cellulosic solids but does not occur in thermoplastics. Instead, other complications such as melting, dripping and bubble formation may occur.) At later times, the decomposition zone begins to develop and then propagate slowly into the solid interior. Cellulosic solids char as they decompose, but thermoplastics may melt and/or bubble and the exposed surface may expand due to entrapped bubbles or regress due to melting and dripping. (Note: to enable in-depth treatment, to the leading order, this work assumes that the solid surface does not regress or expand.) The products of pyrolysis (consisting of combustible volatiles and perhaps moisture) flow out of the hot surface, convecting some of the heat transferred to the solid back into the gas phase. The decomposition, melting and evaporation processes are usually endothermic and

produce an energy sink close to the solid surface. Further, depending on the solid permeability, gas pressures inside the solid may rise. These pressures may force the pyrolysis products both into and out of the solid. Clearly, a multitude of complex physical processes occur as the solid decomposes to produce volatiles. This complexity is, however, surpassed by the relatively unknown decomposition chemistry.

(4) Once the combustible volatiles begin to elute from the solid surface, they mix with the surrounding air in the mass-transfer boundary layer to produce a fuel–air mixture. This mixing process is critical for ignition and depends upon the gas-phase boundary conditions and the manner in which the volatiles elute from the solid surface. For example, ignition may not occur under high-velocity turbulent air conditions. Also, volatiles may eject as localized jets from the solid surface due to internal pressure generation. (In this work, the more common scenario of low volatile injection velocities is assumed.) If the mixing between fuel and air in the boundary layer is assumed to be the same, and if the pyrolysate composition is invariant, then physically the most meaningful ignition criterion would be the critical pyrolysate mass flux. Since pyrolysis products often contain non-combustible or partly combustible components (such as CO_2, H_2O, CO, etc.), it is important to account for their presence because they act as diluents. One obvious method for determining the critical mass flux at ignition is to appropriately correct for the contribution made by the non-combustible components. An alternate and more widely used method is suggested by Rasbash (1975). Here, the effect of diluents is incorporated in determining the heat of combustion per unit mass of the volatiles.

(5) The fuel–air mixture produced in the previous step must be within the flammability limits such that it can be ignited by a pilot flame for piloted ignition. For spontaneous ignition, it must also attain a high enough temperature to produce a gas phase thermal runaway that will subsequently result in a flame. Kashiwagi (1981), through extensive experiments, demonstrated that gas-phase absorption of external radiation is an important mechanism of spontaneous ignition at high radiation fluxes.

(6) Finally, the nascent flame should generate enough heat to overcome the heat losses to the relatively cooler solid surface. Otherwise only momentary flaming or flashes are obtained.

4. Theoretical models

From the above discussion, it is clear that a comprehensive theoretical description of the ignition process is very involved. It requires time-dependent simultaneous solution of the equations describing the complex solid-phase thermal decomposition process and the gas-phase heat and mass-transfer and exothermic reaction processes. Furthermore, there is the following large number of poorly known quantities. (i) The solid-phase decomposition chemistry and the composition of the resulting decomposition products. These are known only for the simplest solids like PMMA. (ii) The thermal and radiative properties of the solid and their changes during decomposition. (iii) The radiation absorption properties of the decomposition products, and their changes with composition. (iv) The chemistry of gas-phase runaway reactions. The obvious complexity of a comprehensive theoretical description has necessitated the development of various empirical ignition criteria discussed above. Thus, the challenge for a theoretical model is to be both simple and realistic. It should include only the essential phenomena, improve our basic understanding and help develop methods

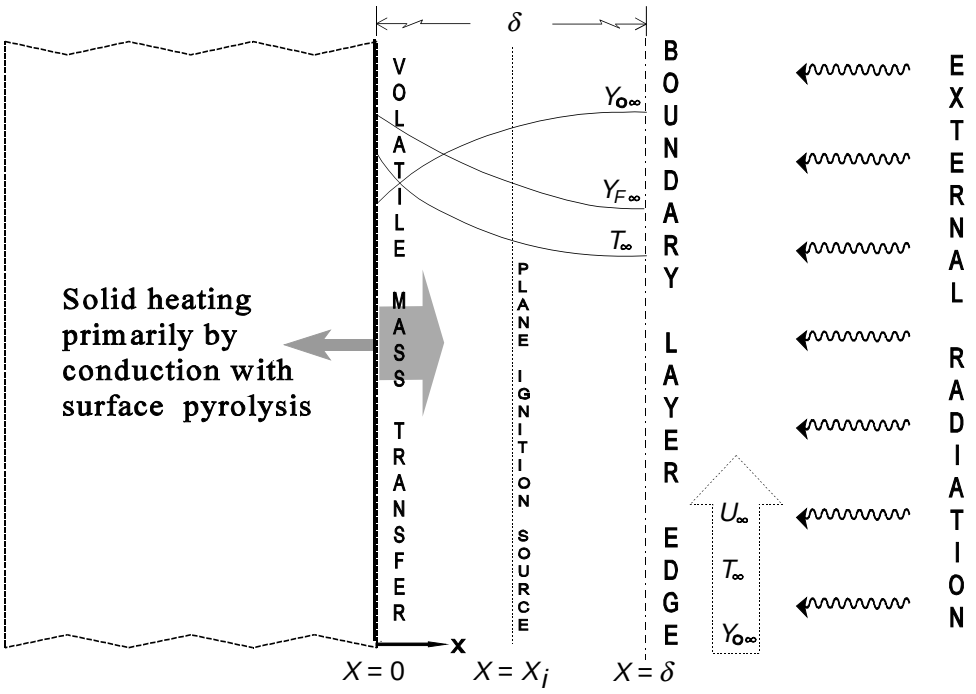

Figure 3. Ignition of solids: the simplified model problem.

for correlating experimental results. The model presented here is based primarily on the work of Kashiwagi (1974) and Gandhi & Kanury (1986) for spontaneous ignition and Tzeng *et al*. (1990), Atreya & Wichman (1989), Rasbash *et al*. (1986) and Atreya & Abu-Zaid (1992) for piloted ignition.

During the ignition process (schematically shown in figure 2), momentum, thermal and mass-transfer boundary layers evolve with time after the commencement of external heating. Clearly, the air flow around the sample, the sample size and shape and its orientation relative to gravity have a major influence on the mixing of air with the evolved fuel volatiles. Since ignition is a local phenomenon, it may be modelled as being one dimensional if the following conditions are satisfied: (i) the characteristic dimension, L, of the solid in the streamwise direction is much larger than the gas-phase diffusion length-scale; (ii) external radiation is uniform over the length-scale L; and (iii) ignition occurs far from the leading edge. Physically, this approximation is justifiable because we are seeking the shortest time required for the appearance of a diffusion flame in the gas phase. Thus, as shown in figure 3, locally the conditions at some distance δ from the slab may be assumed to be maintained constant by a flowing oxidizer stream. For unity Prandtl and Lewis numbers, the boundary layer thickness, δ, is the same for momentum, heat and mass transfers. During transient ignition, two scenarios are possible: (i) either the hydrodynamic boundary layer thickness is established by an external forced convective air flow and thermal and concentration boundary layers develop as the solid is heated; or (ii) both thermal and hydrodynamic boundary layers develop simultaneously in a quiescent atmosphere due to natural convection as the solid is heated and later, as the solid begins to pyrolyse, the concentration boundary layer develops. Both scenarios

may be approximately modelled by assuming a thickness δ which is determined by the outer air flow conditions and the sample dimension L (or Reynolds or Rayleigh numbers assuming unity Prandtl and Lewis numbers). Actually, δ changes with time as $\delta \sim \sqrt{Dt}$, where D is the diffusion coefficient and $t \sim L/U_\infty$ for forced convection and $t \sim (L/g)^{1/2}$ for natural convection. Estimates of this time (for $L \sim 10$ cm; this size is sufficient to approximate an infinite area sample (Simms & Law 1967)) show that the time-scale for transient boundary-layer growth is of the order of 0.1 s, whereas ignition times are much larger than 1 s. Thus, δ is established relatively fast compared to ignition time-scales and may be approximated as a constant during the ignition process. Also, changes in δ may be treated as quasi-steady. This assumption is analogous to using a constant heat-transfer coefficient, which has been frequently assumed in the past. Assuming δ eliminates the gas-phase momentum equation and reduces the problem to the solution of one-dimensional transient continuity, energy and species equations with chemical reactions. This simplified model problem is mathematically tractable and captures the essentials of the ignition phenomenon. It is shown schematically in figure 3.

The above simplification is sufficient for modelling spontaneous ignition. For piloted ignition, however, a model for the pilot source is also required. A typical pilot source has the following characteristics: (i) it must be very small compared to the sample so as to provide negligible amount of heat to the sample; (ii) locally, it must have very high temperatures to initiate gas-phase reactions. These requirements necessitate a three-dimensional model for piloted ignition. Tzeng *et al*. (1990) used an ingenious numerical technique to maintain one dimensionality of the model. They used a plane ignition source placed near the solid in the boundary layer, and to satisfy the condition of negligible heat transfer the ignition source was periodically 'turned on' to test for piloted ignition. If piloted ignition does not occur, the calculations were restarted from the time prior to 'turning on' the pilot source. In this way, the heat supplied by the plane ignition source to the solid becomes negligible.

For the simplest case of constant-pressure ideal-gas reactions with unity Prandtl and Lewis numbers with constant gas- and solid-phase properties, the following governing equations describe both spontaneous and piloted ignition processes.

(*a*) *Gas-phase formulation*

In the gas phase ($0 \leqslant x \leqslant \delta$), the chemical reaction is assumed to be a simple one-step irreversible reaction that follows second-order Arrhenius kinetics with the following stoichiometry:

$$1 \text{ kg fuel} + \nu \text{ kg } O_2 \rightarrow (1+\nu) \text{ kg products} + q \text{ (heat)}. \tag{4.1}$$

The transient governing equations take the form:
continuity,

$$\frac{\partial \rho}{\partial t} + \frac{\partial (\rho v)}{\partial x} = 0; \tag{4.2}$$

energy conservation,

$$\rho \frac{\partial T}{\partial t} + \rho v \frac{\partial T}{\partial x} = \frac{\partial}{\partial x}\left(\frac{\lambda}{c_p}\frac{\partial T}{\partial x}\right) + \frac{1}{c_p}\frac{\partial q_r}{\partial x} + \frac{q}{c_p}\omega; \tag{4.3}$$

fuel conservation,

$$\rho\frac{\partial Y_{\mathrm{F}}}{\partial t}+\rho v\frac{\partial Y_{\mathrm{F}}}{\partial x}=\frac{\partial}{\partial x}\left(\rho D\frac{\partial Y_{\mathrm{F}}}{\partial x}\right)-\omega; \tag{4.4}$$

oxygen conservation,

$$\rho\frac{\partial Y_{\mathrm{O}}}{\partial t}+\rho v\frac{\partial Y_{\mathrm{O}}}{\partial x}=\frac{\partial}{\partial x}\left(\rho D\frac{\partial Y_{\mathrm{O}}}{\partial x}\right)-\nu\omega; \tag{4.5}$$

constant-pressure ideal gas,

$$\rho T=\rho_{\infty}T_{\infty}, \tag{4.6}$$

where the reaction rate or the mass burning rate of the fuel per unit volume ω is given by

$$\omega=A\rho^{2}Y_{\mathrm{F}}Y_{\mathrm{O}}\mathrm{e}^{-E/RT}. \tag{4.7}$$

According to the above definition, the product $A\rho$ has units of s^{-1}.

The symbols used in the above equations are defined in the nomenclature. The last terms in equations (4.3)–(4.5) are the chemical heat release rate and the fuel and O_2 depletion rates, respectively. Also, the term $\partial q_{\mathrm{r}}/\partial x$ in equation (4.3) is the divergence of radiant heat flux and accounts for the gas-phase absorption of radiation with q_{re} being the external radiative heat flux imposed at $x=\delta$. Amos & Fernandez-Pello (1988) assumed the gas-phase absorption of radiation to be proportional to the fuel concentration and the radiation intensity, with the constant of proportionality being the overall absorption coefficient. Their calculations, however, showed that this term is important only for radiant heat fluxes that are much larger than those typically encountered in a fire. Thus, in subsequent calculations this term will be neglected. It is included here for completeness. The initial and boundary conditions are

$$\text{at } t=0,\ 0<x<\delta;\quad Y_{\mathrm{F}}(x,0)=0,\quad Y_{\mathrm{O}}(x,0)=Y_{\mathrm{O}\infty},\quad T(x,0)=T_{\infty}. \tag{4.8}$$

At $t=0$, the radiation source is turned on with an incident irradiance of q_{re}. This results in solid pyrolysis and production of fuel. Thus, the boundary conditions after $t=0$ become, at $x=0$, $t>0$;

$$\rho D\frac{\partial Y_{\mathrm{F}}}{\partial x}\bigg|_{x=0}=\dot{m}''_{\mathrm{S}}(Y_{\mathrm{F}}-Y_{\mathrm{FS}}),\quad \rho D\frac{\partial Y_{\mathrm{O}}}{\partial x}\bigg|_{x=0}=\dot{m}''_{\mathrm{S}}(Y_{\mathrm{O}}),\quad T=T_{\mathrm{S}}, \tag{4.9}$$

where $\dot{m}''_{\mathrm{S}}=(\rho v)_{\mathrm{S}}$, Y_{FS} is the mass fraction of fuel in the volatiles and T_{S} is the surface temperature. These solid–gas interface variables are determined by the heat and mass balance of the solid phase:

$$\text{at } x=\delta,\ t>0;\quad Y_{\mathrm{F}}(\delta,t)=0,\quad Y_{\mathrm{O}}(\delta,t)=Y_{\mathrm{O}\infty},\quad T(\delta,t)=T_{\infty},\quad q_{\mathrm{r}}(\delta,t)=q_{\mathrm{re}}. \tag{4.10}$$

If gas phase absorption of incident radiation is considered, then the solution of the gas-phase equations will yield the value of the incident radiation arriving at the solid–gas interface (q_{rS}). To eliminate this additional coupling of the gas-phase equations with the solid-phase decomposition process, it is convenient to neglect gas-phase absorption of radiation, particularly since it is small at fire-level heat fluxes. With this approximation, $q_{\mathrm{rS}}=q_{\mathrm{re}}$.

(*b*) *Solid-phase formulation*

The variables connecting the gas to the solid phase are $\dot{m}''_{\rm S}, Y_{\rm FS}, T_{\rm S}$ and $q_{\rm rS}$. The first three of these solid–gas interface variables constitute the boundary conditions for the gas-phase model and are determined by the solid-phase model, whereas $q_{\rm rS}$ serves as the boundary condition for the solid-phase model. A simple solid-phase model that is applicable to both cellulosics and thermoplastics, like PMMA, is given below. Several terms in the following equations are simplified when applying this formulation to PMMA.

Mass balance:

$$\frac{\partial \rho_{\rm S}}{\partial t} + \frac{\partial \rho_{\rm m}}{\partial t} = -\frac{\partial \dot{m}''}{\partial x}. \tag{4.11}$$

Here, $\dot{m}''$ is the fuel and moisture mass flux generated by the solid in the positive x-direction with $\dot{m}''(x = 0) = \dot{m}''_{\rm S}$. This mass flux is generated due to change in the solid density ($\rho_{\rm S}$) and change in the moisture content ($\rho_{\rm m}$). For thermoplastics $\rho_{\rm m} = 0$, but for cellulosic materials ignition delay is significantly affected by moisture desorption (Simms & Law 1967; Atreya & Abu-Zaid 1992). For thermoplastics that simply vaporize at the surface (as is often assumed for PMMA), $\dot{m}''_{\rm S} = \rho_{\rm S} v_{\rm S}$, where $v_{\rm S}$ is the linear solid vaporization rate or the surface regression rate.

Energy balance:

$$\underset{[1]}{\rho_{\rm S}\frac{\partial h_{\rm S}}{\partial t}} + \underset{[2]}{\rho_{\rm m}\frac{\partial h_{\rm m}}{\partial t}} + \underset{[3]}{\dot{m}''\frac{\partial h_{\rm g}}{\partial x}} = \underset{[4]}{\frac{\partial}{\partial x}\left(\lambda_{\rm S}\frac{\partial T_{\rm S}}{\partial x}\right)} + \underset{[5]}{\frac{\partial q_{\rm r}}{\partial x}} + \underset{[6]}{(Q_{\rm S} - h_{\rm S} + h_{\rm g})\frac{\partial \rho_{\rm S}}{\partial t}} + \underset{[7]}{(Q_{\rm m} - h_{\rm m} + h_{\rm g})\frac{\partial \rho_{\rm m}}{\partial t}}. \tag{4.12}$$

Here the enthalpy h_i is defined as

$$h_i = \int_{T_\infty}^{T} C_i \, {\rm d}T,$$

where $i = {\rm S}$ (solid), m (moisture), g (gas).

Many terms in the energy equation above can be ignored or simplified. Starting from left to right, (i) the first and the second terms are the rate of increase in enthalpy of the solid and the moisture. The moisture term is zero for PMMA since $\rho_{\rm m} = 0$. For cellulosic materials, it may also be ignored because the moisture content is typically less than 10% and the heat of evaporation is contained in the last term. (ii) The third term accounts for the heat transfer due to volatile mass flow through the solid. This may also be neglected because prior to ignition the volatile mass flux is small and most of the volatiles are generated at or near the surface. (iii) The fifth term accounts for in-depth absorption of radiation by the solid with $q_{\rm rS}$ being the external radiative heat flux arriving at the solid surface. While both cellulosic materials and clear PMMA exhibit in-depth absorption for certain wavelengths of incident radiation and it may affect the ignition delay time (Kashiwagi 1981), often it is adequate to assume that radiation is absorbed at the solid surface. This is because the absorption depth is typically very small (fraction of a millimeter). (iv) The sixth and seventh terms correspond to the energy required for thermal decomposition and

moisture desorption, respectively. The moisture term is clearly zero for PMMA but it may be needed for cellulosic materials depending on the moisture content. The thermal decomposition term may be ignored for cellulosic materials (Atreya 1983*b*) but must be retained for PMMA. However, for PMMA it can be absorbed in the boundary condition if the volatiles are assumed to be generated at the surface, as discussed below.

Decomposition kinetics:

$$\frac{\partial \rho_{\mathrm{S}}}{\partial t} = -A_{\mathrm{S}}(\rho_{\mathrm{S}} - \rho_{\mathrm{Sf}}) \exp(-E_{\mathrm{S}}/RT_{\mathrm{S}}). \tag{4.13}$$

This overall kinetics equation has been used to represent decomposition of cellulosic materials that leave a char residue (ρ_{Sf}). For PMMA, $\rho_{\mathrm{Sf}} = 0$. Also, if the decomposition is approximated to be only at the surface, equations (4.11) and (4.13) can be combined to yield

$$\dot{m}''_{\mathrm{S}} = \rho_{\mathrm{S}} v_{\mathrm{S}} = \bar{A}_{\mathrm{S}} \rho_{\mathrm{S}} \exp(-E_{\mathrm{S}}/RT_{\mathrm{S}}),$$

where $\bar{A}_{\mathrm{S}}$ now has units of velocity. To complete the equations, an expression for the moisture desorption rate ($\partial \rho_{\mathrm{m}}/\partial t$) is also required. Moisture desorption is a complicated process involving internal pressure generation and its detailed description is beyond the scope of the present work. However, for low moisture content typically found in dry wood, it can be well approximated by the following first-order Arrhenius equation (Atreya 1983*a*):

$$\frac{\partial \rho_{\mathrm{m}}}{\partial t} = -A_{\mathrm{m}} \rho_{\mathrm{m}} \exp(-E_{\mathrm{m}}/RT_{\mathrm{S}}), \tag{4.14}$$

where $A_{\mathrm{m}} = 4.5 \times 10^3\ \mathrm{s}^{-1}$, $E_{\mathrm{m}} = 44\ \mathrm{kJ\ mol}^{-1}$ and $Q_{\mathrm{m}} = 2.4\ \mathrm{kJ\ g}^{-1}$. The initial and boundary conditions are

$$\text{at } t = 0,\ -l < x < 0; \quad T_{\mathrm{S}}(x,0) = T_\infty, \quad \rho_{\mathrm{S}}(x,0) = \rho_{\mathrm{S}\infty}, \quad \dot{m}''(x,0) = 0. \tag{4.15}$$

At $x = 0$, $t > 0$, the heat flux into the solid is given by

$$-\lambda_{\mathrm{S}} \frac{\partial T_{\mathrm{S}}}{\partial x}\bigg|_{x=0} = -\lambda \frac{\partial T}{\partial x}\bigg|_{x=0} - \varepsilon\sigma(T_{\mathrm{S}}^4 - T_\infty^4). \tag{4.16}$$

This boundary condition couples the gas- and solid-phase energy equations. However, if the gas-phase absorption of radiation is negligible and if $-\lambda(\partial T/\partial x)|_{x=0}$ can be replaced by $h_{\mathrm{c}}(T_{\mathrm{S}} - T_\infty)$ (where h_{c} is an appropriate heat-transfer coefficient based on the gas-phase Reynolds or Rayleigh numbers, an assumption similar to the boundary layer thickness (δ) assumption already adopted), the solid-phase equations are decoupled from the gas-phase equations and can be solved separately. The gas phase, however, remains coupled to the solid phase and is driven by the solid-phase solution. Further, if external radiation is assumed to be absorbed on the surface rather than in-depth with an absorptivity α ($= \varepsilon$ for a diffuse-grey surface and/or diffuse-grey incident radiation), then the radiation absorption term in equation (4.12) is replaced by the incident heat flux at the boundary. Similarly, if all the decomposition is assumed to occur at the exposed surface, then: (i) for PMMA, the last two terms in equation (4.12) may be replaced by the net heat flux term ($\dot{m}''_{\mathrm{S}} Q_{\mathrm{net}}$) in the boundary condition; and (ii) for cellulosic solids, the moisture term in equation (4.12) is energetically more significant than the decomposition term and must be retained for high moisture content solids (Atreya 1983*a*). However, based

on the work of Simms & Law (1967), moisture effects may be approximated by using appropriately adjusted thermal properties of the solid. If this approximation is adopted for in-depth heat transfer, then the heat of moisture evaporation may be consistently approximated in a manner similar to PMMA. Fortunately, these are excellent approximations at fire level heat fluxes and in the time duration required for ignition. Thus, the heat flux boundary condition (4.16) becomes

$$-\lambda_{\mathrm{S}}\frac{\partial T_{\mathrm{S}}}{\partial x} = \alpha q_{\mathrm{rS}} - h_{\mathrm{c}}(T_{\mathrm{S}} - T_{\infty}) - \varepsilon\sigma(T_{\mathrm{S}}^4 - T_{\infty}^4) - \dot{m}''_{\mathrm{S}}Q_{\mathrm{net}}. \tag{4.17}$$

At $x = -l$, $t > 0$, two boundary conditions are possible depending on the solid thickness l. If l is large, it may be approximated as infinite, yielding $T_{\mathrm{S}}(l \to \infty, t) = T_{\infty}$. However, if l is small or comparable to the thermal thickness $\sqrt{\lambda_{\mathrm{S}} t_{\mathrm{ig}}/\rho_{\mathrm{S}} c_{\mathrm{S}}}$, an appropriate back boundary condition must be used (Beyler 1985). It is important to note that within the approximations made above, the solid phase drives the gas-phase processes. This enhances the importance of the solid-phase model. It is therefore not surprising that several correlations of ignition data in the literature are based primarily on the solution of the solid-phase equations.

(*c*) *Non-dimensional equations and parameters*

The above equations are non-dimensionalized and simplified to obtain relevant parameters for ignition. In the gas phase, the boundary layer thickness δ serves as an appropriate length-scale for non-dimensionalization. Density changes may also be absorbed into this length-scale by introducing the following Howarth transformation:

$$\xi = \frac{1}{\rho_{\infty}\delta}\int_0^x \rho(x,t)\,\mathrm{d}x.$$

Time may be normalized according to the relation $\tau = (\lambda_{\infty}/\rho_{\infty}c_p)t/\delta^2$; or $\tau = D_{\infty}t/\delta^2$ for unity Lewis number. With these transformations, using $\rho^2 D = \rho_{\infty}^2 D_{\infty}$ and neglecting gas-phase absorption of radiation, equation (4.2) is absorbed in the transformation and equations (4.3)–(4.5) become

$$\mathfrak{L}\begin{pmatrix}\theta\\ Y_{\mathrm{F}}\\ Y_{\mathrm{O}}\end{pmatrix} = \begin{pmatrix}Q\\ -1\\ -\nu\end{pmatrix}\mathfrak{R}, \tag{4.18}$$

where

$$\mathfrak{L}(\circ) = \frac{\partial(\circ)}{\partial\tau} + M\frac{\partial(\circ)}{\partial\xi} - \frac{\partial^2(\circ)}{\partial\xi^2}, \qquad \mathfrak{R} = D_{\alpha}Y_{\mathrm{F}}Y_{\mathrm{O}}\exp\left(\frac{-\beta(1-\theta)}{1-\alpha^{\mathrm{o}}(1-\theta)}\right).$$

The definitions of other parameters are as follows: $(\theta = T - T_{\infty})/(T_{\mathrm{f}} - T_{\infty})$, where T_{f} is the adiabatic flame temperature; $M = \dot{m}''_{\mathrm{S}}c_p\delta/\lambda_{\infty}$ is the dimensionless mass flux injected into the boundary layer; $Q = q/(c_p(T_{\mathrm{f}} - T_{\infty}))$ is the normalized heat of combustion; $\alpha^{\mathrm{o}} = (T_{\mathrm{f}} - T_{\infty})/T_{\mathrm{f}}$ is a measure of the heat released (the larger the amount of heat released, the closer α^{o} is to unity); $\beta^{\mathrm{o}} = E/(RT_{\mathrm{f}})$ and

$$\beta = \beta^{\mathrm{o}}\alpha^{\mathrm{o}} = \frac{(T_{\mathrm{f}} - T_{\infty})}{RT_{\mathrm{f}}^2/E}$$

is the Zel'dovich number. The numerator of the Zel'dovich number is a measure of the excess temperature generated by the gas phase chemical reaction and the

denominator is a natural yardstick of reaction temperature. Clearly, if less heat is released by the reaction, it will be more difficult for it to become self-accelerating. Thus, Zel'dovich number measures the ignitability of the gas-phase mixture and is typically around ten for most hydrocarbons. Finally,

$$D_{\mathrm{a}} = \frac{A\rho_\infty \mathrm{e}^{-\beta^o}}{(\lambda_\infty / c_p \rho_\infty \delta^2)}$$

is the gas-phase Damköhler number, which is a ratio of reaction rates to diffusion rates. The reaction rate or the heat generation rate must exceed the heat loss rate for sustained ignition.

The initial and boundary conditions are transformed to:

$$\left.\begin{aligned} &\text{at } \tau = 0,\ 0 < \xi < 1; \quad \theta = 0, \quad Y_{\mathrm{F}} = 0, \quad Y_{\mathrm{O}} = Y_{\mathrm{O}\infty}, \\ &\text{at } \xi = 0,\ \tau > 0; \quad \theta = \theta_{\mathrm{S}}, \quad \frac{\partial Y_{\mathrm{F}}}{\partial \xi} = M(Y_{\mathrm{F}} - Y_{\mathrm{FS}}), \quad \frac{\partial Y_{\mathrm{O}}}{\partial \xi} = M Y_{\mathrm{O}}, \\ &\text{at } \xi = 1,\ \tau \geqslant 0; \quad Y_{\mathrm{F}} = 0, \quad Y_{\mathrm{O}} = Y_{\mathrm{O}\infty}. \end{aligned}\right\} \tag{4.19}$$

The parameters M, Y_{FS} and θ_{S} are obtained from the solution of the solid-phase conservation equations. These equations are simplified by assuming a moisture-free solid and by neglecting in-depth absorption of radiation. As noted above, moisture effects may be incorporated into the thermophysical properties of the solid (Simms & Law 1967; Parker 1988; Janssens 1991) and from the work of Kashiwagi (1974) and Atreya (1983*a*), the effect of net heat of decomposition (Q_{net} in equation (4.17)) on the ignition process is also negligible. It is further assumed that internal heat transfer due to volatile convection is negligible since, during ignition, decomposition occurs primarily in the vicinity of the solid surface. Finally, the solid is assumed to be thick enough to be approximated as semi-infinite with surface absorptivity $\alpha = \varepsilon$. With these approximations, the equations are non-dimensionalized by adopting a length-scale $l = \lambda_{\mathrm{S}\infty} T_\infty / \varepsilon q_{\mathrm{re}}$ and a time-scale $t_{\mathrm{s}} = l^2/(\lambda_{\mathrm{S}\infty}/\rho_{\mathrm{S}\infty} c_{\mathrm{S}})$. The remaining non-dimensional variables are defined as follows:

$$\left.\begin{aligned} \theta^* = \frac{T_{\mathrm{S}} - T_\infty}{T_\infty}, \quad \rho^* = \frac{\rho_{\mathrm{S}}}{\rho_{\mathrm{S}\infty}}, \quad x^* = -\frac{x}{l}, \quad t^* = \frac{t}{t_{\mathrm{s}}}, \\ E^* = \frac{E_{\mathrm{S}}}{RT_\infty}, \quad A^* = A_{\mathrm{S}} t_{\mathrm{s}}, \quad \rho_{\mathrm{f}}^* = \frac{\rho_{\mathrm{Sf}}}{\rho_{\mathrm{S}\infty}}, \quad h^* = \frac{h_{\mathrm{c}} T_\infty}{\varepsilon q_{\mathrm{re}}}, \\ M^* = \frac{\dot{m}_{\mathrm{S}}'' t_{\mathrm{s}}}{\rho_{\mathrm{S}\infty} l}, \quad \sigma^* = \frac{\sigma T_\infty^4}{q_{\mathrm{re}}}, \quad \lambda^* = \frac{\lambda_{\mathrm{S}}}{\lambda_{\mathrm{S}\infty}}. \end{aligned}\right\} \tag{4.20}$$

With these definitions, equations (4.11)–(4.13) become:

mass balance,

$$\frac{\partial \rho^*}{\partial t^*} = \frac{\partial M^*}{\partial x^*}; \tag{4.21}$$

energy balance,

$$\rho^* \frac{\partial \theta^*}{\partial t^*} = \frac{\partial}{\partial x^*}\left(\lambda^* \frac{\partial \theta^*}{\partial x^*}\right); \tag{4.22}$$

decomposition kinetics,

$$\frac{\partial \rho^*}{\partial t^*} = -A^*(\rho^* - \rho_{\mathrm{f}}^*)\mathrm{e}^{-E/(\theta^*+1)}. \tag{4.23}$$

The initial and boundary conditions become

$$\left.\begin{aligned} &\theta^*(x^*,0)=\theta^*(\infty,t)=0, \quad \rho^*(x^*,0)=1, \quad M^*(x^*,0)=M^*(\infty,t)=0,\\ &-\lambda^*\frac{\partial\theta^*}{\partial x^*}\bigg|_{(0,t)}=1-h^*\theta_{\mathrm{S}}^*-\sigma^*[(\theta_{\mathrm{S}}^*+1)^4-1]\equiv\Phi_{\mathrm{S}}. \end{aligned}\right\} \tag{4.24}$$

This solid-phase formulation contains six non-dimensional parameters. Of these, A^*, E^* and ρ_{f}^* control the decomposition kinetics, and λ^*, h^* and σ^* control the surface temperature.

5. Theoretical results and experimental correlations

(*a*) *Spontaneous ignition*

The work of Simms and co-workers (Simms 1960, 1961, 1962, 1963; Simms & Law 1967), Martin (1965) and Alveres & Martin (1971) on spontaneous ignition has been reviewed extensively by Kanury (1972). Thus, greater attention is devoted to more recent work of Kashiwagi (1974), Gandhi *et al*. (1986) and Amos *et al*. (1988), who obtained numerical solutions of the equations discussed in the previous section. Kashiwagi (1974) and Gandhi *et al*. (1986) neglected gas-phase absorption of radiation, whereas that was the primary focus of the work by Amos *et al*. (1988). The models of Kashiwagi (1974) and Gandhi *et al*. (1986) consisted of gas-phase equations (4.1)–(4.7) without the radiation absorption term along with the boundary conditions (4.8)–(4.10). Kashiwagi neglected surface reradiative heat losses and used a similarity transformation, whereas, Gandhi *et al*. adopted a boundary layer thickness, $\delta(t)$, and employed integral solution techniques. In the solid phase, Kashiwagi's model is applicable to thermoplastics like PMMA that pyrolyse at the surface while the model of Gandhi *et al*. is applicable to moisture-free cellulosic materials that pyrolyse in depth. Consequently, moisture terms are dropped in both the models from equations (4.11) and (4.12). In addition, Kashiwagi ignored terms six and seven, while Gandhi *et al*. ignored term five in equation (4.12).

Kashiwagi's calculations show the manner in which the gas-phase temperature profile develops with time during spontaneous ignition. It is interesting that for both the fire level heat fluxes (*ca*. 50 kW m^{-2}) and very high heat fluxes (*ca*. 840 kW m^{-2}) for which the calculations are presented, the surface temperature remains nearly constant during the period in which the gas phase reactions explode. This implies that the contribution of the gas phase exothermic reactions is negligible for raising the surface temperature of the solid. Thus, the critical conditions at ignition are attained primarily by external radiation. This is in agreement with the experimental observation presented in § 2 *c*. Kashiwagi's calculations also show that while the effect of gas- and solid-phase chemical parameters is significant in determining the ignition delay time and the critical conditions at ignition, the calculated results for a given material can be reasonably well correlated by a simple formula based on constant heating of a thermally thick opaque solid (Carslaw & Jaeger 1959) with an assumed constant ignition surface temperature. This constant ignition surface temperature may, however, change with the type of material and its chemical parameters. In terms of the non-dimensional parameters defined in equation (4.20), this simple formula may be expressed as $t_{\mathrm{ig}}^*=t_{\mathrm{ig}}/t_{\mathrm{s}}=\frac{1}{4}\pi\theta_{\mathrm{ig}}^{*2}$. Since θ_{ig}^* is assumed to be constant for a given material, $t_{\mathrm{ig}}^*=$ const. This result is also confirmed by the experimental work

of Simms & Law (1967), who found the correlating temperature to be 545 °C, and Alvares & Martin (1971), who found the correlating temperature to be 600 °C for wood. Simms & Law (1967) correlated their data according to constant heating of a thermally thick opaque solid with linear heat losses, namely

$$t^*_{\rm ig}/\theta^{*2}_{\rm ig} = \eta^2[1 - \exp(\eta^2)\,\mathrm{erf}(\eta)]^{-2}, \quad \text{where } \eta = h^*\sqrt{t^*_{\rm ig}}. \tag{5.1}$$

As the linear heat loss tends to zero, i.e. $h^* \to 0$, the right-hand side of equation (5.1) tends to $\frac{1}{4}\pi$, recovering the previous solution. Note that h^* is a ratio of the convective heat loss coefficient to the absorbed external heat flux. Thus, at low external heat fluxes (*ca.* 20 kW m^{-2}), heat losses become very important and radiative heat loss must also be considered. Typical fire level heat fluxes are around 40 kW m^{-2} and surface temperatures are around 400 °C. This increases the importance of radiative heat losses.

The fact that data can be correlated according to equation (5.1) emphasizes that the inert heating of the solid phase drives the ignition process. The gas- and the solid-phase chemical parameters primarily influence the value of $\theta^*_{\rm ig}$. Kashiwagi's calculations also showed that $\theta^*_{\rm ig}$ increases as $q_{\rm re}$ increases because the flame comes very close to the surface requiring more fuel to sustain the larger heat loss. This is qualitatively in agreement with the criteria for ignition of Rasbash *et al.* (1986).

(*b*) *Piloted ignition*

As mentioned earlier, for building fires, piloted ignition is more important than spontaneous ignition because: (i) it occurs at a lower threshold; (ii) it is the mechanism responsible for fire growth; and (iii) in practice, it is usually impossible to exclude all possible external pilot sources. Drysdale (1985) presents an excellent review of previous work on piloted ignition. Thus, this section will focus on the more recent work.

It is instructive to examine the details of the piloted ignition process. Tzeng *et al.* (1990) numerically solved equations (4.18) along with the boundary conditions (4.19) for the case of specified injection rate of pure CH_4 ($Y_{\rm FS} = 1$) through a porous plate rather than from a pyrolysing solid. Calculations for $\dot{m}'' = 0.834$ g m^{-2} s^{-1}, $T_{\rm S} = T_\infty = 298$ K and $\delta = 1.5$ cm are presented in figure 4*a*, *b*. The difference between the two figures is the location of the igniting pilot. In figure 4*a* the igniting pilot was placed at $\xi = 0.79$ (which corresponds to the theoretically predicted location of the steady diffusion flame), whereas in figure 4*b* the ignition source was at $\xi = 0.13$.

In figure 4*a*, the premixed mixture formed in the boundary layer ignited at $t = 1.089$ s is seen by the sharp temperature peak. The premixed flame then travels quickly into the unburnt mixture in both directions. Thirteen milliseconds later, i.e. at $t = 1.102$ s, the premixed flame consumed nearly all the available oxygen on the fuel side and all the available fuel on the oxidizer side of the ignition source, thereby establishing conditions appropriate for the formation of a diffusion flame. At this time the solid surface experiences a large heat flux (proportional to the temperature gradient), which is probably responsible for the sharp momentary rise in temperature observed during the experiments shown in figure 1. At times larger than 1.102 s, the temperature (and fuel and oxygen concentrations) adjusts slowly to those of a steady diffusion flame, which is finally established at $t = 3.887$ s. Note that its final location is nearly identical to that of the ignition source.

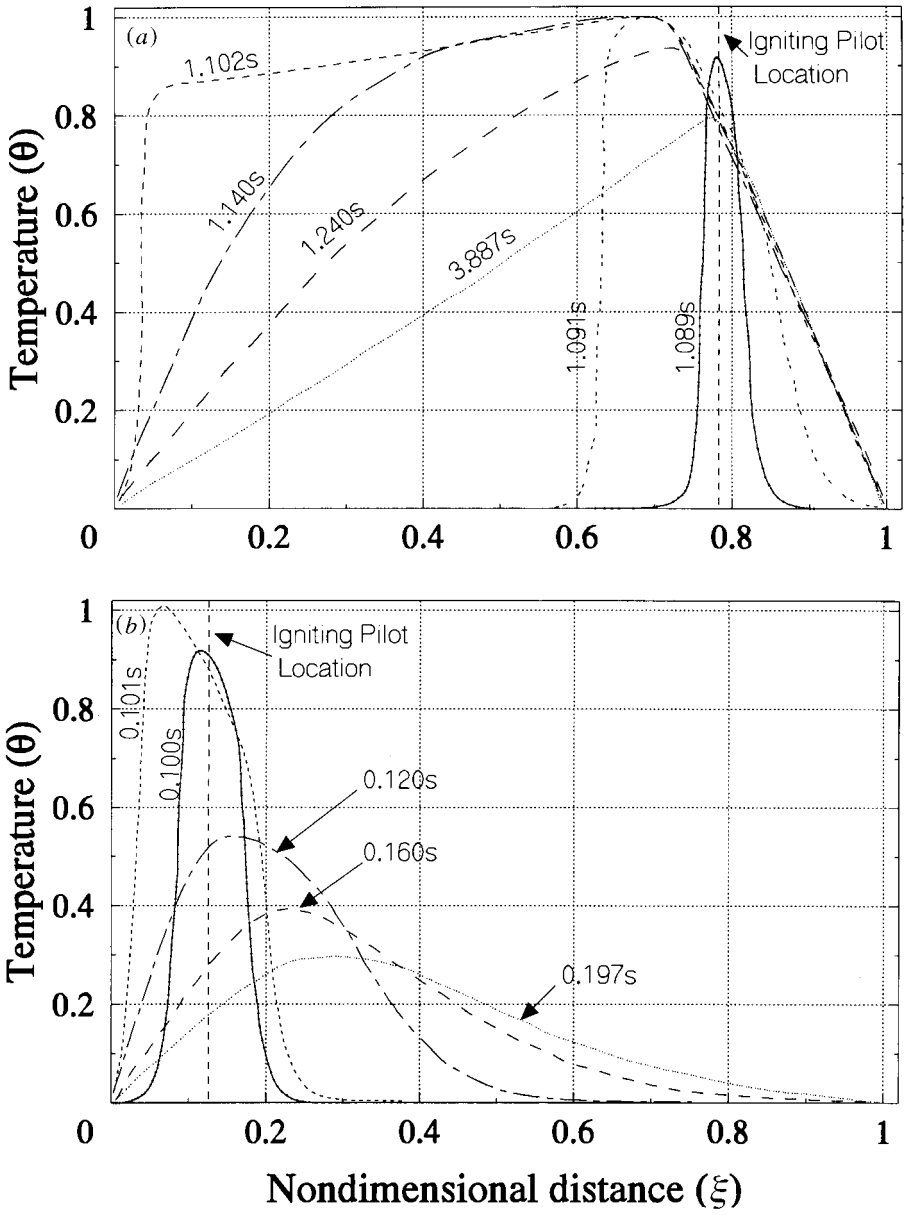

Figure 4. (*a*) Temperature history of sustained piloted ignition from start of ignition to the development of a steady gas-phase diffusion flame at 3.887 s. (*b*) Temperature history of a quenched premixed flame (resulting in a flash).

In figure 4*b*, thermal quenching of the premixed flame prevents the development of a diffusion flame and hence the occurrence of sustained piloted ignition, resulting in a flash. The temperature eventually decays and the fuel and oxygen are subsequently replenished. The gas ignites at 0.1 s (much faster than 1.089 s in figure 4*a*) due to the flammable mixture being formed sooner near the fuel surface. Interestingly, the fuel concentration at the location of the ignition source and at the time of ignition for all

cases was found to be approximately the same ($Y_F \approx 0.044$). This value of Y_F is 80% of the stoichiometric mass fraction and is about 1.74 times the lean flammability limit of CH_4. Similar behaviour was observed if the fuel flow rate falls below the minimum fuel flow rate for piloted ignition.

Clearly, the location of the ignition source is important in determining whether or not sustained piloted ignition will occur. This was observed experimentally by Simms (1963). Numerical calculations show that there exists a minimum location of the ignition source for sustained piloted ignition (comparable to the quenching distance of a premixed flame) regardless of the fuel flow rate. For ignition source distances smaller than the minimum location, the flame is always quenched. As the fuel flow rate is decreased, this minimum location and the theoretical location of the steady diffusion flame approaches each other. Thus, the optimum location of the pilot is the eventual location of the steady diffusion flame.

The minimum fuel flow rate for piloted ignition was determined by placing the igniting pilot at the optimum location. For CH_4 this flow rate was $0.313\ \mathrm{g\ m^{-2}\ s^{-1}}$†. For successful piloted ignition it is necessary to establish a steady diffusion flame. Thus, the minimum fuel flow rate at extinction of a steady diffusion flame is expected to be close to that required for piloted ignition. The minimum fuel flow rate at extinction, as determined by numerical solution of the governing equations, was $0.288\ \mathrm{g\ m^{-2}\ s^{-1}}$ for CH_4. This fuel rate is only about 8% lower than the minimum fuel flow rate for piloted ignition. This result substantiates the hypothesis of Rasbash *et al.* (1986) that conditions at extinction of a steady diffusion flame are similar to those at piloted ignition. This hypothesis was used by Rasbash *et al.* (1986) and Atreya & Wichman (1987, 1989) to obtain an approximate analytical solution for piloted ignition.

While the numerical study of Tzang *et al.* (1990) is very helpful in qualitatively explaining the structure of piloted ignition, it does not help solve the fundamental problem of determining the ignition delay time. Note that with injected fuel, the gas-phase ignition delay times are less than one second. Thus, ignition delay times of several minutes observed in the experiments are entirely a result of the solid-phase processes. This fact has been recognized in the work of Quintiere *et al.* (1983), Quintiere & Harkleroad (1984), Atreya & Wichman (1989), Atreya *et al.* (1986), Thomson & Drysdale (1987), Janssens (1991), Atreya & Abu-zaid (1992) and Drysdale & Thomson (1994), among others.

Atreya (1983*a*) obtained an approximate integral solution of the solid-phase equation (4.22) along with the boundary and initial conditions (4.24). A quadratic tem-

† This is about three times lower than the experimental measurements of Drysdale & Thomson (1989) for hydrocarbon polymers (polyethylene, polypropylene and polystyrene) and about six times lower for oxygenated polymers like PMMA. The probable reasons for the discrepancy between normal hydrocarbon polymers and CH_4 are (i) the assumed gas-phase chemical parameters; and (ii) the choice of an unusually large boundary layer thickness, $\delta = 1.5$ cm. The value of the convective heat transfer coefficient, h_c, often used in the literature is $10\ \mathrm{W\ m^{-2}\ K^{-1}}$. Thus, for average thermal conductivity of air, $0.05\ \mathrm{W\ m^{-1}\ K^{-1}}$, $\delta \sim 0.5$ cm. Note that in equations (4.18) and (4.19), the fuel flow rate, $\dot{m}''$, enters the equations only through the parameter M. Thus, for all other conditions and parameters remaining constant, $\dot{m}'' \sim 1/\delta$, recovering the factor-of-three difference between the measurements of Drysdale & Thomson (1989) for hydrocarbon polymers and the calculations of Tzeng *et al.* (1990) for CH_4. While this close agreement may be fortuitous, it seems to indicate that the details of the gas-phase chemical kinetics (not thermochemistry) may be unimportant for piloted ignition due to the presence of the high temperature pilot flame.

perature profile,

$$\theta^*(x,t) = \theta_S^{*2}(t^*)(1 - x^*(\Phi_S/\theta_S^*) + x^{*2}(\Phi_S^2/4\theta_S^{*2})),$$

was used for the purpose. This solution was later used by Atreya & Wichman (1987, 1989) to establish a relationship between the critical surface temperature and the critical fuel mass flux at piloted ignition. Further, by using the criteria for extinction of a diffusion flame, they determined the critical fuel mass flux at ignition, thus providing a predictive model for piloted ignition. The integral solution of equations (4.22) and (4.24) yields

$$\frac{t^*}{\theta_S^{*2}} = \frac{1}{3}\left(\frac{1}{\Phi_S^2} - \frac{10AB}{\theta_S^*(A^2-4B)^2} - \frac{2(A+2B\theta_S^*)}{\theta_S^*(A^2-4B)\Phi_S}\right), \tag{5.2}$$

where $A = -(h^* + 4\sigma^*)$, $B = -25\sigma^*/3$.

This equation shows excellent agreement with the experimental surface temperature data for wood prior to ignition (Atreya 1983*a*). Using equation (5.2) and assuming that $\rho^* \approx 1$ during piloted ignition (i.e. valid only during the initial stages of the decomposition process), equations (4.21) and (4.23) are integrated to yield the pyrolysis mass flux, M_S^*, as

$$M_S^* = \frac{A^*(1-\rho_f^*)}{\Phi_S E^*}(\theta_S^*+1)^2 e^{-E^*/(\theta_S^*+1)}\left(1 - \frac{\exp[-E^*(\theta_S^*/(\theta_S^*+1)]}{(\theta_S^*+1)^2}\right). \tag{5.3}$$

Equation (5.3) shows that $M_S^*(\theta_S^* = 0) = 0$, and that M_S^* increases exponentially with increasing $\theta_S^*(t)$. More importantly, it relates the surface temperature at the time of ignition (θ_S^*) to the pyrolysis mass flux, M_S^*. Now, following Rasbash *et al.* (1986), the minimum fuel mass flux required to sustain a diffusion flame is obtained from the gas-phase energy balance as

$$M_S^* = \frac{Y_{O\infty} c_S h^*(\theta_f^* - \theta_S^*)/\nu c_p}{[\Delta H - \theta_f^* - Y_{O\infty}(\theta_f^* - \theta_S^*)/\nu]}, \tag{5.4}$$

where ΔH ($= (Y_{O\infty}/c_p T_\infty \nu) \times$ (heat of combustion)) is the normalized heat of combustion of air which is approximately constant for most hydrocarbons ($\Delta H \approx 9.25$, with $c_p = 1.12\ \mathrm{J\ kg^{-1}\ K^{-1}}$ and $T_\infty = 20\ ^\circ\mathrm{C}$) and $\theta_f^* = (T_f - T_\infty)/T_\infty$ is the normalized flame temperature. For a given fuel, $Y_{O\infty}/\nu$ is also constant and for wood the value is *ca.* 0.23 (Atreya 1983*a*). Physically, the right-hand side of equation (5.4) is the ratio of the heat lost by the flame to the sample surface divided by the excess combustion heat available after accounting for the heat required to bring both the fuel and the air to the flame temperature T_f. The only unknown in equation (5.4) is the flame temperature (T_f) at the extinction of a diffusion flame. Given T_f and the material properties, M_S^* can be related to θ_S^* with h^* as a parameter. Fortunately, the work of Ishizuka & Tsuji (1981) shows that near extinction the flame temperature is remarkably constant for most hydrocarbons and is about 1550 K (see also Beyler 1983). Thus, with these approximations, equations (5.2)–(5.4) provide a unique solution for the piloted ignition problem. They relate the time, surface temperature and volatile mass flux at ignition to the conditions of the experiment and the solid- and gas-phase thermal and chemical properties. Once the surface temperature and the mass flux is obtained from the simultaneous solution of equations (5.3) and (5.4), time to ignition may be calculated from equation (5.2). Figure 5 shows a graphical solution of these equations.

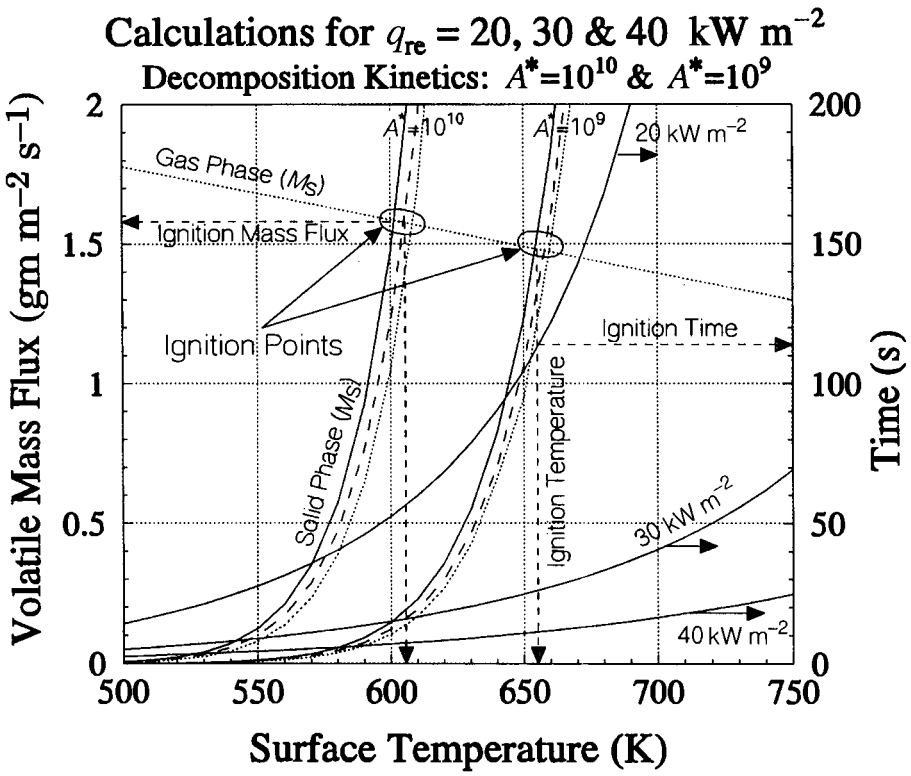

Figure 5. A graphical solution of equations (5.2)–(5.4) to predict surface temperature, fuel mass flux and time at piloted ignition.

In figure 5, the calculations were done for wood for three different levels of external radiation (q_{re} = 20, 30 and 40 kW m^{-2}) and two different values of the non-dimensional pre-exponential factor A^* in equation (5.3). The values of other properties, taken from various handbooks, were $\varepsilon = 0.85$, $\rho_f^* = 0.25$, $c_S = 1.38$ J g^{-1}K^{-1}, $\rho_{S\infty} = 500$ kg m^{-3}, $E = 122.5$ J g^{-1}mol^{-1}, $T_\infty = 293$ K, $h_c = 10$ W m^{-2} K^{-1}, $Y_{O\infty} = 0.23$, $\nu = 1$ and $c_p = 1.12$ J g^{-1}K^{-1}. The curves labelled solid phase (M_S) are obtained from equation (5.3), whereas the curves labelled gas phase (M_S) are obtained from equation (5.4). In each case, three curves are produced for three different values of external radiation. Since gas phase (M_S) does not depend on external radiation and A^*, all the curves coincide. The intersection of these curves is the ignition point which yields a unique solution for the fuel mass flux and the surface temperature at piloted ignition. The corresponding time to ignition is obtained from equation (5.2), which is also plotted in figure 5.

It is interesting to note that the predicted ignition temperatures lie within the measured range of 325–375 °C. The critical fuel mass flux, however, is somewhat lower than that measured by Deepak & Drysdale (1983), Bamford *et al.* (1946) and Atreya & Abu-Zaid (1992). The curves labelled solid phase (M_S) show that the prediction is very sensitive to decomposition kinetics and for a given set of kinetic parameters, the surface temperature and the critical fuel mass flux at ignition are essentially independent of the external heat flux. This confirms the constant surface

temperature and constant volatile mass flux ignition criteria. The ignition delay predictions, on the other hand, are very sensitive to the external heat flux and the surface heat losses, as evident from the temperature–time curves in figure 5. It is, however, important to remember that this solution is valid for negligible thermal decomposition prior to ignition. Thus, it is more accurate for larger heat fluxes.

The above model, while limited to a moisture-free idealized solid with well-known decomposition kinetics, confirms two previously known important facts that can be used for developing correlations for other materials. These are (i) surface temperature incorporates most the effects of decomposition kinetics and may be assumed constant at ignition; and (ii) an inert solid solution may be used for determining the ignition delay, as long as surface heat losses are correctly accounted. These facts have been recognized by Quintiere *et al*. (1983), Quintiere & Harkleroad (1984), Atreya & Wichman (1989), Atreya *et al*. (1986), Janssens (1991, 1992), Atreya & Abu-zaid (1992) and Drysdale (1994), among others, to develop data correlation methods and determine the minimum heat flux at piloted ignition.

Atreya & Abu-zaid (1992) rewrote equation (5.2) explicitly in terms of surface heat losses by noting that for a constant surface temperature at ignition ($\theta^*_{\rm ig}$) the last two terms inside the bracket on the right-hand side are very weakly dependent on the external heat flux contained in $\Phi_{\rm S}$, and expressing $\Phi_{\rm S} = 1 - L/\varepsilon q_{\rm re}$. Thus, equation (5.2) may be rewritten as

$$\frac{t^*_{\rm ig}}{\theta^{*2}_{\rm ig}} = \frac{e(q_{\rm re}, L)}{3\Phi^2_{\rm S}}, \quad \text{where } \frac{L}{\varepsilon q_{\rm re}} = h^*\theta^*_{\rm ig} + \sigma^*[(\theta^*_{\rm ig}+1)^4 - 1] = L^*. \tag{5.5}$$

Here, $e(q_{\rm re}, L)$ is a very weak function of the external heat flux ($q_{\rm re}$) and the surface heat losses (L). For fire level heat fluxes (between 30 and 60 kW m^{-2}) it is almost constant and decreases by about 10% at 20 kW m^{-2}. Since e does not depend on material properties, equation (5.5) may be used to correlate experimental data for any material. In dimensional terms, equation (5.5) can be written as

$$q_{\rm re} = Ct^{-1/2}_{\rm ig} + L/\varepsilon, \quad \text{where } C = \sqrt{\frac{(\lambda_{\rm S\infty} c_{\rm S} \rho_{\rm S\infty})e}{3\varepsilon^2}}\theta_{\rm ig}. \tag{5.6}$$

This simple equation is very useful because chemical and physical parameters that influence ignition are clearly delineated and related to the measured ignition time and the imposed external heat flux. Thus, data can be correlated according to the straight line ($t^{-1/2}_{\rm ig}$) versus ($q_{\rm re}$). Here L, which has been identified as the heat loss, becomes the intercept and C is the slope of the straight line. Note that L/ε ($\equiv q_{\rm cr}$) is the critical incident heat flux below which ignition is impossible (or $t_{\rm ig} \to \infty$) and C contains the moisture-dependent thermal properties of the solid and $\theta_{\rm ig}$ which depends on the decomposition chemistry. A more accurate expression was obtained by Janssens (1992), who solved numerically equations (4.22) and (4.24) and correlated the results according to $t^{0.547}_{\rm ig}$ instead of $t^{1/2}_{\rm ig}$. Janssens (1991) also conducted numerous experiments in the cone calorimeter and correlated his results in this manner to obtain the critical incident heat flux at ignition ($q_{\rm cr} = L/\varepsilon$).

Data plotted according to equation (5.6) are shown in figure 6*a*, *b* along with the least-squares-fit lines. These data are taken from Atreya & Abu-zaid (1992), who varied experimentally the environmental parameters such as air velocity and ambient oxygen concentration and the physical properties of wood by changing its moisture content. Thus, the effect of environmental variables on both L and C in

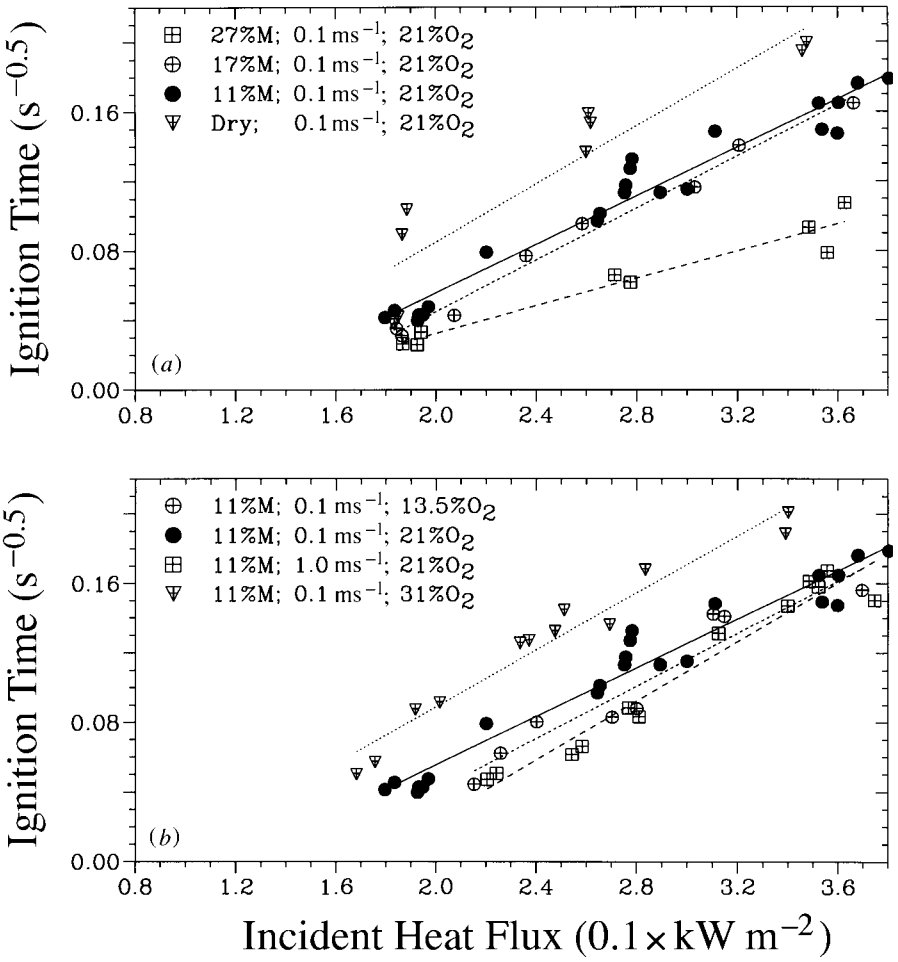

Figure 6. Data plotted according to equation (5.6) along with the least-square-fit lines. (*a*) Correlation for the effect of moisture content. (*b*) Correlation for the effect of air velocity and O_2%.

equation (5.6) was investigated. In both parts of figure 6, experiments with 11% moisture (% dry weight), 0.1 m s^{-1} air velocity and 21% O_2 represent normal room conditions. Figure 6*a* shows the effect of changing the moisture content from dry to 27% while holding all other conditions constant. It appears that small changes in the moisture content (from 11 to 17%) fall within the experimental error and sample-to-sample property variations, thus the data for 11% and 17% may be considered at an average 14% moisture content. From figure 6*a* it is clear that changing the moisture content affects the slope of the correlating straight lines due to changes in the thermal properties and θ_{ig}. The intercept or the critical incident heat flux at ignition ($q_{cr} = L/\varepsilon$) also shows some variation with moisture content (10–12 kW m^{-2}). This may be because of several reasons. (i) Theoretically, the heat required to evaporate moisture will appear as a surface heat loss in the integral formulation used to derive

equation (5.2). While it is difficult to estimate the value of this heat loss because the moisture evaporation rate decreases as wood is dried prior to ignition, a larger value of q_{cr} would be expected for larger moisture content. (ii) In reducing equation (5.2) to (5.5), C, L and θ_{ig} at ignition were assumed to be constant. These are not true constants. (iii) At low heat fluxes, long exposures result in a build-up of low thermal conductivity char layer prior to ignition. This was not considered in deriving the model.

Figure 6*b* shows the effect of changing the air velocity and the oxygen concentration. This is expected to primarily affect the surface heat loss and therefore the critical incident heat flux. As seen, the correlating lines have nearly the same slope but different intercepts. The heat loss depends on the convective heat transfer coefficient and θ_{ig}, which increase with air velocity (0.1–1 m s^{-1}) and decrease in the oxygen concentration (31–13.5%).

6. Conclusions

In this paper an attempt has been made to summarize the state-of-the-art understanding of the combined physics of heat and mass transfer and the chemistry of solid-phase decomposition and gas-phase runaway reactions that lead to ignition. A general theoretical model valid for both vaporizing and charring materials is presented and specific numerical and analytical solutions are discussed in the light of experimental evidence and data.

For piloted ignition, it seems that the details of the multistep gas-phase chemistry may be less important than decomposition chemistry due to the ever present high-temperature piloted ignition source in the gas phase. Decomposition chemistry also dictates the gas-phase thermochemistry and stoichiometry that play a very important role. Since most of the thermal decomposition during ignition occurs near the surface, it is reasonable to expect a strong correlation of the ignition data with surface temperature assuming that the decomposition chemistry remains unaltered. If the decomposition chemistry and ambient conditions stay constant, surface temperature and mass flux at ignition are also expected to be constant. Under these conditions, the volatile mass flux is uniquely related to the surface temperature through equation (5.3). The successful correlation of the ignition delay data by a simple thermal model based on inert heating of the solid (within the assumption of constant surface temperature) supports this hypothesis. A corollary to this is that if the surface temperature at ignition is not constant under constant ambient conditions, decomposition chemistry must be varying and a significantly more complicated description of the solid-phase decomposition will be necessary. Fortunately this is not the case for most materials. It may be further extrapolated that effective fire retardants must work by altering the solid-phase decomposition chemistry. Recent results of Drysdale & Thomson (1994) seem to concur with this hypothesis. These results show that while the surface temperature and mass flux at ignition remain constant for both unretarded and fire-retarded thermoplastics, they are significantly increased in the fire-retarded configuration. This implies that the decomposition chemistry stays constant in both configurations but changes significantly due to fire retardants. A better understanding of the decomposition chemistry will be necessary for developing new fire retardants.

For spontaneous ignition, on the other hand, the details of the multistep gas-phase chemistry are likely to be very important in addition to the decomposition chemistry because the gas-phase runaway reactions must self-initiate. As an example, for methane the gas-phase decomposition reaction ($CH_4 \rightleftharpoons CH_3 + H$) will play an important role along with the chain branching reactions (such as $H + O_2 \rightleftharpoons O + OH$). This complicates the modelling of spontaneous ignition.

The author thanks the National Institute of Standards & Technology and NASA for continuing support of his fire-related research under the program direction of Dr David D. Evans and Dr Kurt R. Sacksteder.

Nomenclature

A	pre-exponential constant for the gas-phase Arrhenius reaction ($m^3\ kg^{-1}\ s^{-1}$)
c_p	specific heat of the gas at constant pressure ($kJ\ kg^{-1}\ K^{-1}$)
c_S	specific heat of the solid ($kJ\ kg^{-1}\ K^{-1}$)
D	diffusion coefficient ($m^2\ s^{-1}$)
ΔH	non-dimensional heat of combustion of air
E	activation energy ($kJ\ kmol^{-1}$)
h_c	convective heat transfer coefficient ($kW\ m^{-2}\ K^{-1}$)
L	characteristic length of the sample in the streamwise direction (m), also heat loss ($kW\ m^{-2}$)
l	sample thickness
$\dot{m}''$	volatile mass flux ($kg\ m^{-2}\ s^{-1}$)
M	non-dimensional volatile mass flux
q	heat of combustion per unit mass of fuel ($kJ\ kg^{-1}$)
Q	heat of solid decomposition or moisture desorption ($kJ\ kg^{-1}$)
q_r	radiative heat flux ($kW\ m^{-2}$)
q_{re}	external incident heat flux ($kW\ m^{-2}$)
R	universal gas constant ($8.314\ kJ\ kmol^{-1}\ K^{-1}$)
T	temperature (K)
t	time (s)
v	gas velocity ($m\ s^{-1}$)
x	coordinate normal to the surface (m)
Y_i	mass fraction of species i
α	absorptivity
δ	boundary layer thickness (m)
ε	emissivity
λ	thermal conductivity ($W\ m^{-1}\ K^{-1}$)
ν	stoichiometric oxygen-to-fuel ratio by mass (kg/kg)
Φ	net non-dimensional heat flux into the solid
ρ	gas density ($kg\ m^{-3}$)
σ	Stefan–Boltzmann's constant ($5.67 \times 10^{-8}\ W\ m^{-2}\ K^{-4}$)
θ	non-dimensional temperature
τ	non-dimensional time

ω reaction rate or the mass burning rate of the fuel per unit volume (kg m^{-3} s^{-1})

subscripts

e external
F fuel
f flame, or final value
g gas
ig at ignition
∞ ambient value
m moisture
O oxidizer
re external radiation
S solid or at the solid surface

superscripts

* non-dimensional quantity

References

Abu-Zaid, M. 1988 Effect of water on piloted ignition of cellulosic materials. PhD thesis, Michigan State University, USA.

Agrawal, S. & Atreya, A. 1992 Wind-aided flame spread over an unsteadily vaporizing Solid. In *24th Symp. (Int.) on Combustion*, pp. 1685–1693. Pittsburgh, PA: The Combustion Institute.

Akita, K. 1959 Studies on the mechanisms of ignition of wood. *Rep. Fire Res. Inst. Jap.* **9**, 1–44.

Alvares, N. J. & Martin, S. B. 1971 Mechanisms of ignition of thermally irradiated cellulose. In *13th Symp. (Int.) on Combustion*, pp. 905–914. Pittsburgh, PA: The Combustion Institute.

Amos, B. & Fernandez-Pello, A. C. 1988 Model of the ignition and flame development on a vaporizing combustible surface in a stagnation point flow: ignition by vapor fuel radiation absorption. *Combust. Sci. Technol.* **62**, 331–343.

ASTM 1990*a* Standard test method for heat and visible smoke release rates for materials and products using an oxygen consumption calorimeter. E 1354-90. Philadelphia, PA: American Society for Testing and Materials.

ASTM 1990*b* Standard test method for determining material ignition and flame spread properties. E 3121-90. Philadelphia, PA: American Society for Testing and Materials.

Atreya, A. 1983*a* Pyrolysis, ignition and fire spread on horizontal surfaces of wood. PhD thesis, Harvard University, USA.

Atreya, A. 1983*b* Heat of decomposition in wood pyrolysis. In *Proc. of the Eastern Section of The Combustion Institute*, pp. 27–30. Pittsburgh, PA: The Combustion Institute.

Atreya, A. & Abu-Zaid, M. 1992 Effects of environmental variables on piloted ignition. In *3rd Int. Symp. Fire Safety Sci.* **3**, 177–186.

Atreya, A. & Wichman, I. S. 1987 Heat and mass transfer during piloted ignition of cellulosic materials. In *Proc. ASME–JSME Thermal Engng Joint Conf.*, vol. 1, pp. 433–440.

Atreya, A. & Wichman, I. S. 1989 Heat and mass transfer during piloted ignition of cellulosic materials. *J. Heat Transfer* **111**, 719–725.

Atreya, A., Carpentier, C. & Harkleroad, M. 1986 Effects of sample orientation on piloted ignition and flame spread. *1st Int. Symp. Fire Safety Sci.*, **1**, 97–109.

Babrauskas, V. & Parker, W. 1987 Ignitability measurements with the cone calorimeter. *J. Fire Mater.* **11**, 31–43.

Bamford, C. H., Crank, J. & Malan, D. H. 1946 The combustion of wood. I. *Proc. Camb. Phil. Soc.* **42**, 166–182.

Beyler, C. L. 1983 The interaction of a buoyant diffusion flame with a hot vitiated layer. PhD thesis, Harvard University, USA.

Beyler, C. L. 1985 Ignition properties of materials. Report to IBM. Borehamwood, UK: Fire Research Station.

Carslaw, H. S. & Jaeger, J. C. 1959 *Conduction of heat in solids*, 2nd edn. Oxford University Press.

Deepak, D. & Drysdale, D. 1983 Flammability of solids: an apparatus to measure the critical mass flux at the firepoint. *Fire Safety Jl* **5**, 167–169.

Drysdale, D. D. 1985 *Introduction to fire dynamics*, pp. 206–221. New York: Wiley.

Drysdale, D. D. & Thomson, H. E. 1989 Flammability of plastics. II. Critical mass flux at the firepoint. *Fire Safety Jl* **14**, 179–188.

Drysdale, D. D. & Thomson, H. E. 1994 Ignitability of flame retarded plastics. *4th Int. Symp. Fire Safety Sci.* **4**, 195–204.

Gandhi, P. D. & Kanury, A. M. 1986 Criteria for spontaneous ignition of radiantly heated organic solids. *Combust. Sci. Technol.* **50**, 233.

Ishizuka, S. & Tsuji, H. 1981 An experimental study of effect of inert gases on extinction of laminar diffusion flames. In *18th Symp. (Int.) on Combustion*, pp. 695–703. Pittsburgh, PA: The Combustion Institute.

ISO 1990 Rate of heat release from building products. International Standards Organization, DIS 5660. Geneva: ISO.

Janssens, M. L. 1991 Fundamental thermophysical characteristics of wood and their role in enclosure fire growth. PhD thesis, University of Gent.

Janssens, M. L. 1992 A thermal model of piloted ignition of wood including variable thermophysical properties. In *3rd Int. Symp. Fire Safety Sci.* **3**, 167–176.

Kanury, A. 1972 Radiative ignition mechanism of solid fuels. A review. *Fire Res. Abstr. Rev.* **14**, 24–52.

Kanury, A. 1988 Flaming ignition of solid fuels. *SFFE handbook of fire protection engineering* (ed. P. DiNenno), pp. 326–340. Quincy, MA: National Fire Protection Association.

Kashiwagi, T. 1974 A radiation ignition model of a solid fuel. *Combust. Sci. Technol.* **8**, 225–236.

Kashiwagi, T. 1979 Effects of attenuation of radiation on surface temperature for radiative ignition. *Combust. Sci. Technol.* **20**, 225–230.

Kashiwagi, T. 1981 Radiative ignition mechanism of solid fuels. *Fire Safety Jl* **3**, 185–200.

Kashiwagi, T. 1982 Effect of sample orientation on radiative ignition. *Combust. Flame* **44**, 223–245.

Koohyar, A., Welker, J. & Sliepcevich, C. 1968 The irradiation and ignition of wood by flame. *Fire Technol.* **4**, 284–291.

Martin, S. 1965 Diffusion-controlled ignition of cellulosic materials by intensive radiant energy. In *10th Symp. (Int.) on Combustion*, pp. 877–896. Pittsburgh, PA: The Combustion Institute.

Mekki, K., Atreya, A., Agrawal, S. & Wichman, I. 1990 Wind-aided flame spread over charring and non-charring solids: an experimental investigation. In *23rd Symp. (Int.) on Combustion*, pp. 1701–1707. Pittsburgh, PA: The Combustion Institute.

Parker, W. J. 1988 Prediction of the heat release rate of wood. PhD thesis, The George Washington University, Washington, DC.

Quintiere, J. G. 1981 A simplified theory for generalizing results from a radiant panel rate of flame spread apparatus. *J. Fire Mater.* **5**, 52–60.

Quintiere, J. G. 1995 Surface flame spread. In *SFPE handbook of fire protection engineering*, pp. 205–216. Quincy, MA: National Fire Protection Association.

Quintiere, J. G. & Harkleroad, M. 1984 New concepts for measuring flame spread properties. NBSIR 84-2943, Gaithersubrg, MD.

Quintiere, J., Harkleroad, M. & Walton, D. 1983 Measurement of material flame spread properties. *Combust. Sci. Technol.* **32**, 67–89.

Rasbash, D. 1975 Relevance of fire point theory to the assessment of fire behaviour of combustible materials. *Int. Symp. on Fire Safety of Combustible Materials, Edinburgh University.*

Rasbash, D. & Drysdale, D. D. 1983 Theory of fire and fire processes. *J. Fire Mater.* **7**, 79–88.

Rasbash, D., Drysdale, D. D. & Deepak, D. 1986 Critical heat and mass transfer at pilot ignition and extinction of a material. *Fire Safety Jl* **10**, 1–10.

Robertson, A., Gross, D. & Loftus, J. 1956 A method for measuring surface flammability of materials using a radiant energy source. *ASTM Proc.*, vol. 56, 1437–1456.

Sauer, F. 1956 Ignition of black a-cellulose papers by thermal radiation. Report AFSWP-869. Madison, WI: USDA Forest Service.

Simms, D. L. 1960 Ignition of cellulosic materials by radiation. *Combust. Flame* **4**, 293–300.

Simms, D. L. 1961 Experiments on the ignition of Cellulosic materials by thermal radiation. *Combust. Flame* **5**, 369–375.

Simms, D. L. 1962 Damage to cellulosic solids by thermal radiation. *Combust. Flame* **6**, 303–318.

Simms, D. L. 1963 On the pilot ignition of wood by radiation. *Combust. Flame* **7**, 253–261.

Simms, D. L. & Law, M. 1967 The ignition of wet and dry wood by radiation. *Combust. Flame* **11**, 377–388.

Smith, W. K. & King, J. B. 1970 Surface temperature of materials during radiant heating to ignition. *J. Fire Flammability* **1**, 272–288.

Steward, F. R. 1974 Ignition characteristics of cellulosic materials. *Heat transfer in fires* (ed. P. Blackshear), pp. 379–407. New York: Wiley.

Thomson, H. E. & Drysdale, D. D. 1987 Flammability of plastics. *Fire Mater.* **11**, 163–172.

Thomson, H. E., Drysdale, D. D. & Beyler, C. 1988 An experimental evaluation of critical surface temperature as a criterion for piloted ignition of solid fuels. *Fire Safety Jl* **13**, 185–196.

Tzeng, L. S., Atreya, A. & Wichman, I. S. 1990 A one-dimensional model of piloted ignition. *Combust. Flame* **80**, 94–107.

Weatherford, W. D. & Sheppard, D. M. 1965 Basic studies of the mechanisms of ignition of cellulosic materials. In *10th Symp. (Int.) on Combustion*, pp. 897–910. Pittsburgh, PA: The Combustion Institute.

Welker, J. R. 1970 The pyrolysis and ignition of cellulosic materials: a literature review. *J. Fire Flammability* **1**, 12–29.

Wesson, H. R., Welker, J. R. & Sliepcevich, C. M. 1971 The piloted ignition of wood by thermal radiation. *Combust. Flame* **16**, 303–310.

PHILOSOPHICAL TRANSACTIONS OF THE ROYAL SOCIETY A MATHEMATICAL, PHYSICAL & ENGINEERING SCIENCES